Neomorphic *agouti* mutations in obese yellow mice

David M. J. Duhl[1], Harry Vrieling[1], Kimberly A. Miller[1], George L. Wolff[2] & Gregory S. Barsh[1]

Several dominant mutations of the mouse *agouti* coat colour gene have pleiotropic effects that include obesity and a yellow coat. The A^{y} allele is caused by a large deletion that affects the expression of several contiguous genes. We show that three other obesity-associated *agouti* mutations, A^{iy}, A^{sy} and A^{vy}, are due to different molecular alterations that result in ubiquitous expression of a chimaeric RNA that encodes a normal agouti protein. The A^{iy} and A^{vy} alleles are caused by insertion of an intracisternal A particle element 1 kb or 100 kb, respectively, upstream of agouti coding sequences. These results provide a model for other genes that show allele-specific imprinting, and demonstrate that molecular mechanisms typically responsible for activation of proto-oncogenes can also lead to other disease phenotypes.

[1]*Department of Pediatrics and Howard Hughes Medical Institute, Stanford School of Medicine, Stanford, California 94305, USA*
[2]*National Center for Toxicological Research, Food and Drug Administration, U.S. Department of Health and Human Services, Jefferson, Arkansas 72079, USA*

H.V. present address: MGC Department of Radiation Genetics and Chemical Mutagenesis, Wassenaarseweg 72, 2333 AL Leiden, The Netherlands

Correspondence should be addressed to G.S.B.

Single-gene mutations in animals can provide useful models for understanding the pathophysiology of multifactorial human diseases. The lethal yellow (A^{y}) and *viable yellow* (A^{vy}) mutations of the mouse *agouti* locus are dominant pleiotropic mutations resulting in a yellow coat, increased tumour susceptibility and adult-onset obesity[1–4] (reviewed in refs 5,6). Two other *agouti* locus mutations, *intermediate yellow* (A^{iy}) and *sienna yellow* (A^{sy}), also result in dominant inheritance of a yellow coat and obesity[7,8]. Similar to most forms of human obesity, increased adiposity in yellow mice is more hypertrophic then hyperplastic[9], occurs in parallel with increases in lean body mass[10,11], and is associated with insulin resistance and, especially in males, diabetes[12,13]. Hyperphagia develops in mutant animals beginning at 3–4 weeks of age, but peripheral changes in energy metabolism are also thought to play a role in obesity associated with *agouti* locus mutations[14–17].

Unlike most other *agouti* mutations, expressivity of A^{vy} is variable and subject to parental imprinting effects[18]. Most animals that carry A^{vy} are obese and have a variegated coat colour phenotype in which an underlying pattern of transverse yellow stripes are interrupted at irregular intervals by patches of black or brown hair (Fig. 1). However, some animals exhibit somatic reversion for both obesity and coat colour. Reversion to the lean pseudoagouti phenotype is more likely to occur in animals who inherit A^{vy} paternally than those who inherit A^{vy} maternally, but is also dependent on strain background[11]. Neither coat colour variegation nor parental imprinting have been described in animals that carry A^{iy}, A^{sy} or A^{y}, but, like A^{vy}, apparent somatic reversion occurs frequently in A^{iy} (ref. 7).

Mice that carry A^{y} and A^{vy} have been studied intensely, but the molecular mechanisms that underlie altered regulation of body weight remain unclear. We and others have recently cloned the *agouti* gene[19,20], which appears to encode a small secreted protein that normally causes melanocytes within hair follicles to switch from the synthesis of black or brown to yellow pigment. Genomic and cDNA cloning studies suggest the A^{y} mutation was caused by a large deletion that lies at least 100 kb centromere-proximal to *agouti* coding sequences[21,22]. One consequence of this deletion is the ubiquitous expression of chimaeric mRNAs containing *agouti* protein-coding sequences[19–22]. However, the complex nature of the mutation, combined with a lack of knowledge regarding the allele of origin, has made it difficult to distinguish whether A^{y}-associated obesity is caused by ectopic expression of a normal agouti protein, expression of a fusion protein with a novel activity, or a coincidental and closely linked molecular lesion that is independent of abberant *agouti* expression. Comparison of A^{y} to other *agouti* mutations is also complicated by its effects on embryonic development — unlike A^{iy}, A^{sy} and A^{vy}, animals homozygous for A^{y} die shortly before implantation[22,23].

To examine the relationship of *agouti* gene expression to the pleiotropic phenotype observed in mice that carry A^{iy}, A^{sy} and A^{vy}, we have performed RNA expression and molecular cloning studies of these mutations. Remarkably, we find that each of the three alleles is associated with ubiquitous expression of *agouti* coding sequences due to different molecular alterations that result in the production of chimaeric RNAs with unique 5' ends. In the case of A^{vy}, the nature of the new 5' sequences suggests possible mechanisms for variable expressivity and parental origin effects.

Fig. 1 Variable expressivity and mottling associated with the A^{vy} mutation. The C57BL/6J-A^{vy}/a mice are genetically identical and 3–4 months of age. The phenotypes shown left to right are obese yellow, obese mottled, and lean pseudoagouti. Pseudoagouti animals almost always inherit A^{vy} paternally rather than maternally[18], and differ from the non-mutant agouti phenotype in that individual hairs show a disordered pattern of pigment deposition.

Ectopic expression of *agouti* in A^{iy}, A^{sy} and A^{vy}

The normal *agouti* RNA is approximately 800 nucleotides (nt) in length, derived from a primary transcript that contains four or five exons, and, after birth, is expressed in the skin only during the short time that yellow pigment is being produced. In contrast, chimaeric RNAs associated with the A^{y} mutation are slightly longer due to the addition of new 5' sequences and are expressed in nearly every tissue of the body. To determine the size and tissue distribution of *agouti* RNAs in other obesity-associated *agouti* alleles, a northern blot that contained total RNA prepared from different tissues of adult A^{sy}/a, A^{iy}/A^{iy}, yellow A^{vy}/a, or pseudoagouti A^{vy}/a mice was hybridized to a cDNA probe that contained *agouti* exons 2–4. This probe detected an RNA of approximately 1000 nucleotides in brain, spleen, kidney, liver, heart and skin of A^{sy}/a, A^{iy}/A^{iy}, and yellow A^{vy}/a animals, but only in the lung and the skin of pseudoagouti A^{vy}/a animals (Fig. 2). A more sensitive reverse transcription-PCR (RT-PCR) assay detected expression of *agouti* coding sequences in all tissues of pseudoagouti A^{vy}/a animals (data not shown), but expression detectable by northern hybridization to total RNA was observed only in the lung of one of three animals examined. These results provide evidence that, as in the case of A^{y}, mutations that result in dominant inheritance of a yellow coat and obesity are associated with ubiquitous expression of RNA that contains *agouti* coding sequences. The level of expression associated with A^{iy} is approximately 2–5 fold less then that associated with A^{sy} and A^{vy}, which correlates with the relative degree of obesity caused by these mutations[2,7].

To determine the protein-coding potential of the ectopically expressed *agouti* RNAs, we used a PCR-based method[25] to isolate partial cDNA clones from spleen RNA in which the 3' end of each clone was reverse transcribed and amplified by oligonucleotide primers within *agouti* exons 3 and 2, respectively. The *agouti* protein-coding sequence in exon 2 is normally preceded by one of four alternative exons, 1A, 1A', 1B, or 1C (Fig. 3*a*). Of 13 clones that were isolated and sequenced, all contained the normal *agouti* translational initiation site in exon 2 and had unchanged *agouti* coding sequences, but differed in the nature of their 5' sequences. Two new classes of 5' sequences

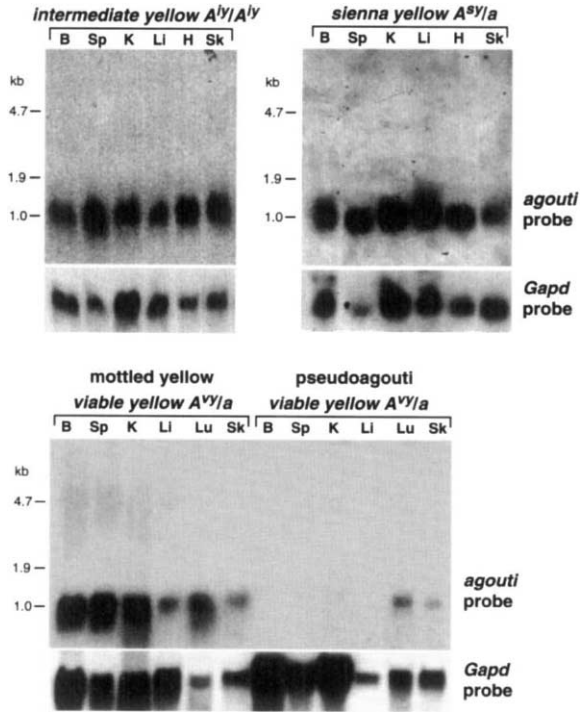

Fig. 2 Northern hybridization analysis of the A^{iy}, A^{sy} and A^{vy} alleles. 30 μg of total RNA from the brain (B), spleen (Sp), kidney (K), liver (Li), lung (Lu), heart (H) or skin (Sk) of an adult A^{iy}/A^{iy}, A^{sy}/a, yellow A^{vy}/a or pseudoagouti A^{vy}/a animal was fractionated by formaldehyde/agarose electrophoresis, transferred to a nylon membrane and hybridized with an *agouti* cDNA probe that contained exons 2–4. After hybridization, the filter was stripped and rehybridized with a Glyceraldehyde 3-phosphate dehydrogenase (*Gapd*) probe to check that approximately equivalent amounts of RNA were in each lane. The *a* allele was used opposite A^{sy} and A^{vy} because there is no detectable expression of *agouti* RNA in tissues of *a/a* mice[24]. In A^{iy}/a animals, *agouti* expression was barely detectable, and therefore A^{iy}/A^{iy} animals were used for the experiment depicted here. The blots shown are representative of additional experiments in which three animals of each type were examined; expression of *agouti* RNA has also been observed in A^{iy}/A^{iy} and A^{sy}/a lung, and in yellow A^{vy}/a heart; however, expression in pseudoagouti A^{vy}/a lung was observed in only one animal.

were isolated from A^{iy}/a mice, a third was isolated from A^{sy}/a mice and a fourth was isolated from A^{vy} mice (Fig. 3*b*). In the A^{iy} and A^{sy} cDNAs, the 5' sequence diverges from the non-mutant sequence precisely at the splice acceptor site that precedes exon 2 (Fig. 3*b*). Of the 152 nts that precede exon 2 in the A^{vy} cDNA, residues 57–152 are nearly identical to a portion of *agouti* exon 1A, which normally lies at the 5' end of isoforms specific for the ventral region of the body in *light-bellied agouti* (A^{W}) and *black-and-tan* (a^{t}) alleles[26], but residues 1–56 are novel (Fig. 3*d*). In the discussion that follows, the 5' ends of the ectopically expressed cDNAs are referred to as exon 1(A^{iy}1), exon 1(A^{iy}2), exon 1(A^{sy}) and exon 1(A^{vy}). Because none of these exons contain an open reading frame with an ATG predicted to initiate translation[27], and none are capable of producing a fusion protein with sequences in exon 2, 3 or 4, the effects shared in common by A^{iy}, A^{sy}, A^{vy}, and A^{y} are likely to be mediated by ectopic expression of a normal agouti protein.

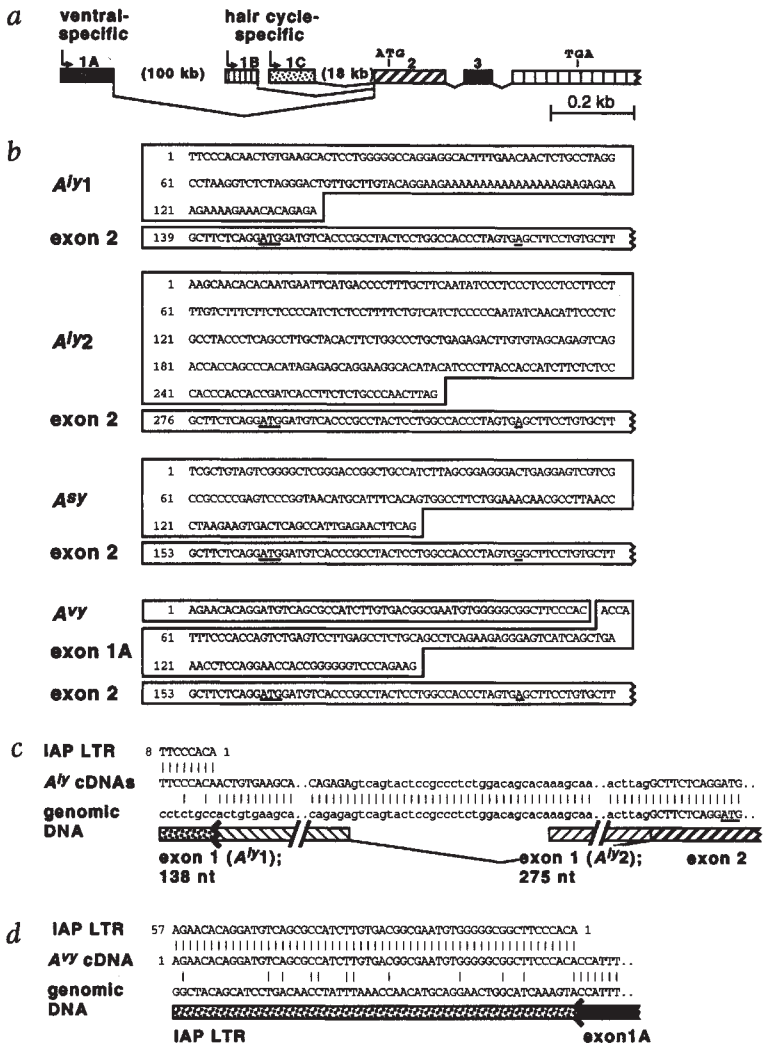

Fig. 3 cDNA cloning analysis of the A^{iy}, A^{sy} and A^{vy} alleles. *a*, Exon structure of the non-mutant *A* allele. Exon 1A initiates *agouti* isoforms specific for ventral skin, while exons 1B or 1C initiate isoforms expressed in both ventral and dorsal skin, but only during the mid-portion of the hair growth cycle. Not shown is an alternatively spliced exon that we have previously described in the A^{W} allele, exon 1A'[26]. *b*, Total RNA from spleen of an adult A^{iy}/A^{iy}, A^{sy}/a or a yellow A^{vy}/a animal was used as the substrate for RACE cloning (see Methodology). The number of clones isolated and sequenced for the A^{iy}1, A^{iy}2, A^{sy} and A^{vy} classes was 2, 1, 6 and 4, respectively. Among members of a single class, all clones ended within 10–20 nts of each other; in each case, the sequence shown represents the longest clone obtained. The translational initiation site in exon 2 is underlined as is a A/G polymorphism that results in a Ser to Gly substitution in the signal sequence. *c*, Sequence similarity between exon 1 (A^{iy}) cDNA clones, genomic sequences immediately 5' to exon 2, and 8 nts at the 5' end of an IAP long terminal repeat[29]. Exon 1 (A^{iy}*1*) uses a cryptic splice donor within the intron, CAGAGAlgtcagt; exon 1 (A^{iy}*2*) is colinear with genomic DNA. *d*, Sequence similarity between exon 1 (A^{vy}), exon 1A and 57 nts at the 5' end of an IAP long terminal repeat[29]. Residues 57–152 of the A^{vy} cDNA are identical to the sequence previously cloned from the A^{W} allele except for the insertion of a G residue at position 140 of the A^{vy} cDNA. For both A^{iy} and A^{vy}, the IAP-like sequences are identical to those from an IAP element inserted within the IL-3 gene[29], and correspond to the reverse complement of the U3 segment[28].

A^{iy}, A^{sy} and A^{vy} lesions affect 5' end of *agouti*

Comparison of the A^{iy}1 and A^{iy}2 cDNA sequences to other portions of the *agouti* gene revealed that exon 1(A^{iy}1) and exon 1(A^{iy}2) each contain genomic sequences that are normally removed by RNA processing (Fig. 3*c*). Exon 1(A^{iy}2) contains 275 nts of genomic DNA that lie immediately upstream of exon 2 including the splice acceptor sequences normally used by exon 2. Exon 1(A^{iy}1) lies 28 nts further upstream and therefore makes use of a cryptic splice donor within intron 1 to produce the A^{iy}1 cDNA. Exon 1(A^{iy}1) is colinear with genomic DNA except for the first 8 of 138 nts, which are identical to a segment from the long terminal repeat of an intracisternal A particle (IAP) element (Fig. 3*c*)[28,29]. Likewise, the novel sequences in exon 1(A^{vy}), residues 1–56, are identical to an IAP long terminal repeat (Fig. 3*d*). The fusion between the IAP sequences and those in exon 1(A^{iy}*1*) or exon 1 (A^{vy}) cDNA does not occur in a region of genomic DNA that contains a potential splice acceptor site. Instead, insertion of an IAP element directly into exon 1A or just upstream of exon 2 is likely to be responsible for production of the A^{vy} or A^{iy} cDNAs, respectively.

To characterize more precisely these molecular abnormalities, we used oligonucleotide primers that flanked the suspected IAP insertion sites to amplify genomic DNA from A^{vy}/a or A^{iy}/a animals (Fig. 4*a*). Primers close to exon 1A amplified the expected product of 306 bp from all DNA samples, but amplified an additional fragment approximately 5.4 kb in length from A^{vy}/a DNA.

Likewise, primers close to exon 2 amplified the expected product of 648 bp from all DNA samples, but amplified a 5.4 kb fragment from A^{iy}/a DNA. Further characterization of the 5.4 kb fragments revealed IAP LTR sequences at both insertion junctions with direct repeats in genomic DNA of 6 bp (Fig. 4*b*). Full-length IAP elements are 7.1 kb long, but internal deletions and small insertions previously described in cloned IAP elements can be used to distinguish several families approximately 4–5 kb in length[30]. The location of *Bam*HI, *Eco*RI, *Sac*I and *Xba*I restriction sites within the inserted DNA recovered from A^{vy}/a animals corresponds to those expected for a type IΔ1 IAP element[30] with a transcriptional orientation opposite that of *agouti* (Fig. 4*b*), and is consistent with the orientation of the LTRs as determined by sequence analysis. Taken together, these observations indicate that the A^{iy} and A^{vy} mutations were caused by insertion of IAP elements, such that transcription of the A^{iy} and A^{vy} cDNAs occurs in a direction opposite to that used normally for IAP RNAs. In the case of A^{vy}, insertion directly into exon 1A produces a chimaeric cDNA in which the normal *agouti* splice site pattern is preserved; but in the case of A^{iy}, insertion into an intron produces a chimaeric cDNA which makes use of a cryptic splice donor ($A^{iy}1$). The 5' end of the $A^{iy}2$ cDNA is colinear with intron sequences immediately upstream of exon 2, and additional studies will be required to determine whether its transcriptional initiation site may lie within the IAP LTR. An IAP element with bidirectional promoter activity is also thought to be responsible for activation of the *c-mos* gene in a mouse plasmacytoma[31,32], but A^{iy} and A^{vy} represent the first examples we are aware of in which insertional activation by a retrotransposon has caused an inherited mutation in mice.

Unlike A^{iy} and A^{vy}, the 152 nucleotide segment that comprises exon 1 (A^{sy}) is not similar to any sequence in the public databases and, when used as a probe, does not hybridize with a 150 kb contig of cloned DNA that spans the entire *agouti* locus[26] (data not shown). However, Southern hybridization experiments to genomic DNA from A^{iy}/a and A^{sy}/a mice with three probes (b, c and d) that span the 17 kb region between *agouti* exon 1B and the Ba*m*HI site immediately upstream of exon 2 reveal a single *Bam*HI fragment of altered mobility in A^{sy} DNA (Fig. 5), suggesting that A^{sy} is caused by an insertion of novel DNA approximately 10–15 kb 5' of *agouti* exon 2. The *Bam*HI fragments detected by probes b, c and d are not altered in A^{iy}/a DNA (Fig. 5), indicating that the A^{iy} IAP insertion characterized by sequence analysis (Fig. 4) affects only the *Bam*HI fragment that contains exon 2.

In A^{vy}/a DNA, a probe that contains a portion of exon 1A (probe a in Fig. 5), detects 3.5 kb, 10 kb and 11 kb fragments; comparison to *a/a* DNA indicates that the 10 kb fragment is specific for A^{vy}, and has arisen from a 7 kb fragment evident in *A/A* DNA (*A* is the allele of origin for A^{vy}). Probe a is part of a partial duplication, but in studies to be described elsewhere, we have determined that the portion of exon 1A contained within the A^{vy} cDNA lies on the 7 kb and not the 11 kb *Bam*HI fragment. The positions and nature of the A^{iy}, A^{sy} and A^{vy} mutations, and the

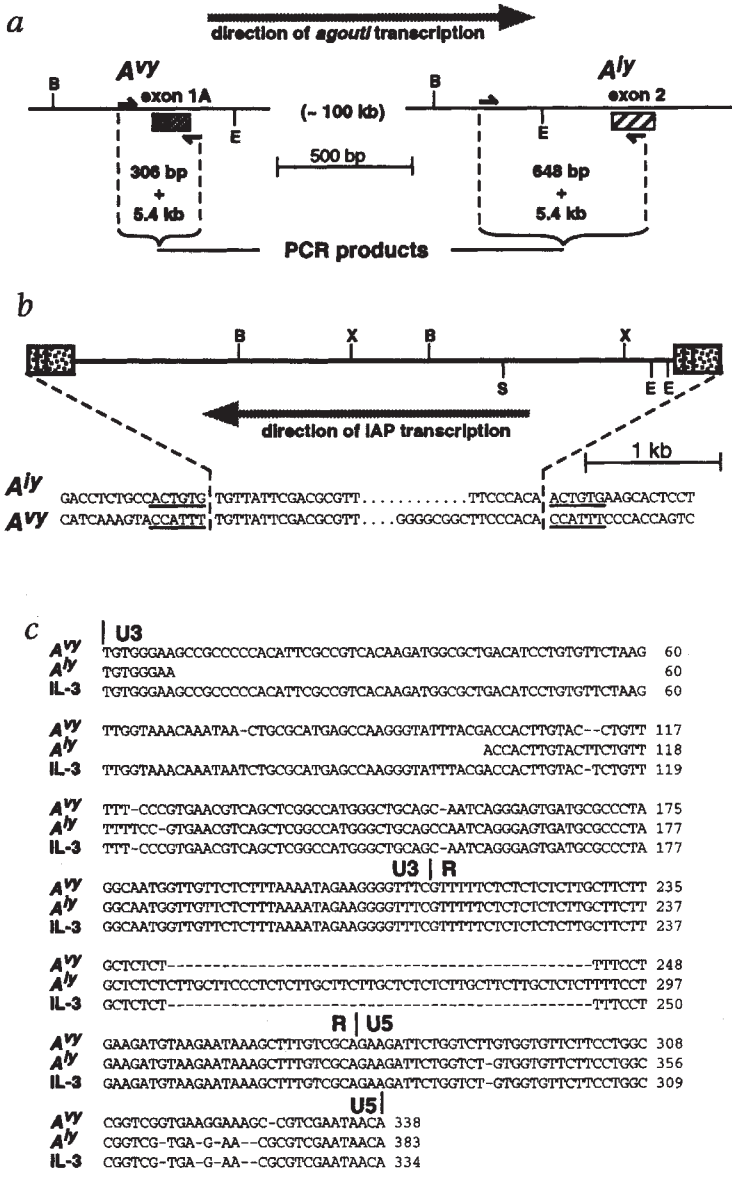

Fig. 4 Characterization of the IAP elements in A^{iy} and A^{vy} genomic DNA. *a*, Oligonucleotide primers that flanked the predicted insertion sites as indicated in Fig. 3*c,d* were used to amplify PCR products of approximately 5.4 kb from the A^{iy} or A^{vy} allele. PCR products of this size were observed only with the indicated combinations of alleles and primer pairs. A "sense" primer within intron 1, 5'–AGCCTTTATCCTTCGTCCTTC–3', and an "antisense" primer within exon 2, 5'–CGAGTTCATGGAGGAGT-TACTCCGC–3', are located 648 apart, and were used to amplify A^{iy}/a genomic DNA. A "sense" primer upstream of exon 1A, 5'–AAGCCACCACACAACACAGA–3', and a "antisense" primer at the splice donor of exon 1A, 5'–GAGTTTAGCACATACCTTCT–3', are located 306 nt apart, and were used to amplify A^{vy}/a genomic DNA. The approximate locations of these primers are indicated relative to exon 1A, exon 2 and genomic *Bam*HI (B) or *Eco*RI (R) sites. *b*, Restriction map of the A^{vy} IAP element, and sequence of the IAP insertion junctions for A^{iy} and A^{vy}. Direct repeats at the site of insertions are underlined and were determined by comparison to the sequence of genomic DNA from the *A* allele. *c*, Comparison of LTR sequences from the A^{iy}, A^{vy} and IL-3[29] IAP elements. Dashes have been introduced to maximize the similarity among the three LTRs; a gap is present where the sequence has not been determined for a portion of the U3 segment in A^{iy}.

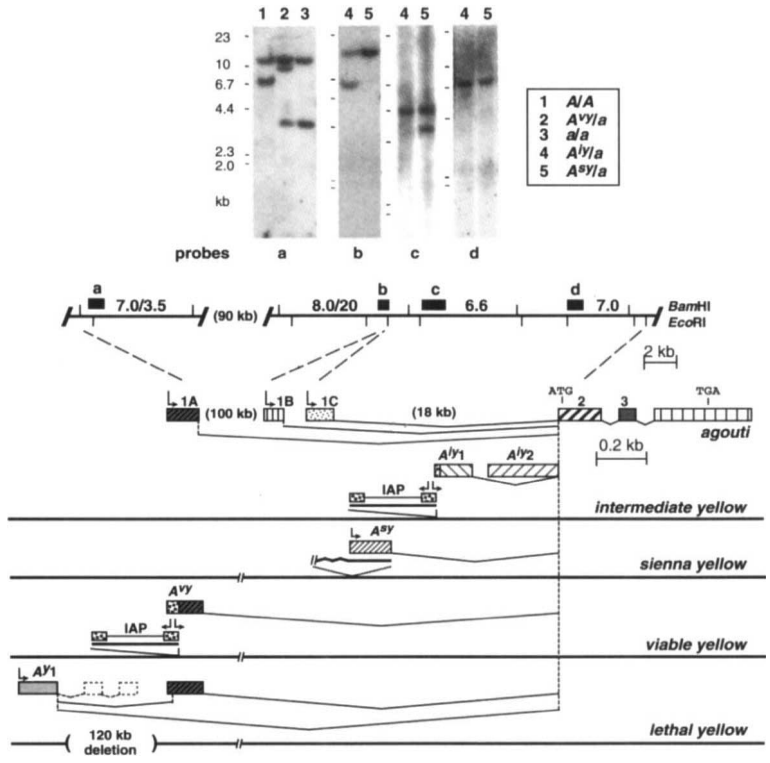

Fig. 5 Genomic Southern hybridization analysis of the A^{iy}, A^{sy} and A^{vy} alleles, and summary of molecular alterations in obesity-associated *agouti* alleles. In the upper panel, genomic DNA from C3H/HeJ-*A/A*, C57BL/6J-A^{vy}/*a*, C57BL/6J-*a*/*a*, C57BL/6J-A^{iy}/*a* or C57BL/6J-A^{sy}/*a* mice was digested with *Bam*HI and hybridized with the indicated probes. The mobilities of molecular weight markers listed at the left-hand edge of the autoradiograph are indicated with horizontal lines immediately adjacent to each panel. Probe a is a 0.4 kb genomic *Pst*I–*Xho*I fragment that contains a portion of exon 1A; it detects 3.5 kb, 7.0 kb, and 10 kb *Bam*HI fragments specific for the *a*, *A*, and A^{vy} alleles, respectively; probe a also detects an 11 kb *Bam*HI fragment common to all three alleles due to a partial duplication whose structure will be described elsewhere. Probe b is a 0.5 kb *Stu*I–*Eco*RI genomic fragment that contains exons 1B and 1C; it detects 8.0 kb and 20 kb *Bam*HI fragments specific for the *A* and *a* alleles, respectively. A^{iy}/*a* mice are heterozygous for the 8.0 kb and 20 kb fragments because A^{iy} arose from the *A* allele; A^{sy}/*a* mice are homozygous for the 20 kb fragment because A^{sy} arose from the *a* allele. Probe c is a 2.5 kb genomic *Eco*RI–*Nco*I fragment within intron 1 that detects a 6.6 kb *Bam*HI fragment in the *a* allele but a 5.0 kb *Bam*HI fragment specific for the A^{sy} allele. Probe d is a 1.0 kb genomic *Xba*–*Apa*I fragment within intron 1 that detects a 7.0 kb *Bam*HI fragment in all *agouti* alleles examined. A restriction map, sizes of the internal *Bam*HI fragments cloned from the *A* allele (or the variant fragments specific for the *a* allele), and location of probes a–d are shown below the autoradiograph. The lower panel shows a summary of molecular alterations in obesity-associated *agouti* alleles. The normal exon structure of the *A* allele is shown on the top line, in which *agouti* isoforms can be initiated with one of three different first exons. As described in the text, insertions of IAP elements or novel DNA are responsible for A^{iy}, A^{sy} or A^{vy}. The molecular alteration responsible for A^{y} is a 120 kb deletion described in ref. 22.

previously described A^{y} mutation[22], are summarized in the bottom portion of Fig. 5, and indicate that alterations of genomic DNA that lie approximately 1, 10, 100 and 200 kb upstream of *agouti* exon 2 are responsible for the abnormal cDNAs produced by the A^{iy}, A^{sy}, A^{vy} and A^{y} alleles.

Discussion

Adult-onset obesity and a yellow coat are two components of the pleiotropic phenotype observed in mice that carry one of four dominant mutations of the *agouti* locus[6]. The molecular defect previously described in one of these mutations — a 120 kb deletion associated with the A^{y} mutation — affects the expression of at least two genes, *Raly* and *agouti*[21,22]; but the results presented here indicate that ectopic expression of *agouti* is responsible for the effects shared among A^{iy}, A^{sy}, A^{vy} and A^{y}. Besides an effect on metabolism and somatic growth, mice that carry A^{vy} or A^{y} also exhibit small but significant increases in susceptibility to a wide variety of tumours[3,4,33–36]. Our results suggest a similar effect is likely to occur in mice that carry A^{iy} or A^{sy}.

IAP elements as a cause of hereditary mutations. The two obesity-associated *agouti* mutations caused by IAP insertions, A^{iy} and A^{vy}, both arose on a C3H/HeJ - *A/A* background[2,7], and the sizes and LTR sequences of the inserted elements are similar. IAP elements are expressed widely during early embryonic development but in restricted tissues in the adult animal[29,37]. Factors that control IAP transposition are not well understood; however, IAP element diversity among different strains of mice indicates that new insertions have occurred frequently during the derivation of inbred strains[38,39]. Although it is possible that the *agouti* locus is a "hotspot" for IAP integration, it seems more likely that it is one of a small class of genes that, when expressed ubiquitously, leads to a phenotype which is easily visible yet still compatible with reproduction.

Apparent somatic reversion — the lean pseudoagouti phenotype — occurs frequently in A^{iy} and A^{vy}, and therefore is likely to be mediated by sequences within the IAP elements. Using RT-PCR, we detected low levels of *agouti* expression in all tissues of pseudoagouti A^{vy}/*a* mice. This suggests that epigenetic inactivation of regulatory sequences within the IAP LTR rather than excision of the IAP explains somatic reversion in A^{iy}/– and A^{vy}/– mice, and is consistent with the observation that neither allele exhibits germline reversion. Somatic reversion has not been well-characterized for A^{iy}, but in the case of A^{vy}, genetic studies show that the likelihood of reversion depends on both strain background and parental origin. For example, the frequencies of complete somatic reversion (the pseudoagouti phenotype) were 1% or 12% in VY/Wf-A^{vy}/*a* animals who inherited A^{vy} from their mother or father, respectively; but the corresponding frequencies in AT/Wf-A^{vy}/a^{t} animals were 4.9% or 24.6%, respectively[18]. These effects are likely to be mediated by strain-specific modifier genes that control expression of the IAP LTR, in some cases independently in each parent.

Both A^{iy} and A^{vy} were caused by IAP insertions into a chromosome bearing an *A* allele, therefore the observation that A^{vy} but not A^{iy} exhibits coat colour variegation may be related to the different sites of insertion. Exon 1A, the site of the A^{vy} insertion, is normally expressed at significant levels in the *light-bellied agouti* (A^{W}) but not the A allele, and therefore may lie in an area of chromatin that is

transcriptionally inactive. In contrast, the site of the A^{iy} insertion is very close to exon 2, which is used in both ventral-specific and hair cycle-specific *agouti* isoforms[26]. An interesting parallel to A^{vy} variegation is observed in the *chinchilla-mottled* (c^m) mutation, in which genetic modifiers have been identified and in which clonal inheritance of tyrosinase activity is maintained by changes in chromatin conformation[40].

***Agouti* mutations and genetic obesity.** Deregulated expression of a normal gene product is a well-recognized cause of non-heritable diseases that occur in somatic tissues, but this type of mutational mechanism is a less common cause of inherited disorders. Since the wild-type *agouti* gene does not regulate body weight, partial or complete loss-of-function mutations affect pigment deposition but not adiposity. Thus, even though mutations similar in nature to those that activate proto-oncogenes could account for genetic obesity in many different mammals, polymorphic variations in *agouti* expression are unlikely to cause a significant proportion of obesity in most populations.

Nonetheless, the recognition that *agouti*-associated obesity is caused by ectopic expression of a normal signalling molecule suggests that the underlying biochemical mechanism may shed light on processes that normally regulate body weight in mice and in humans. One model, based on the opposing effects of agouti protein and alpha-melanocyte stimulating hormone (α-MSH) on pigment production in hair follicles, is that the agouti protein binds to one or more melanocortin receptors expressed in the central nervous system, thereby antagonizing the effects of α-MSH and related molecules[41]. An alternative hypothesis is that agouti binds to its own, as yet unidentified receptor, which activates an independent signal transduction pathway and interferes with the action of α-MSH at an intracellular level[5,42]. Distinguishing among these alternatives will lead to a better understanding of signalling pathways that normally regulate body weight in all mammals.

Methodology

Mouse strains and mutations. The A^{iy} and A^{vy} mutations arose spontaneously in the C3H/HeJ-*A*/*A* strain and the A^{sy} mutation arose spontaneously in the C57BL/6J-*a*/*a* strain[8]. Mice carrying A^{iy} (B6.C3H-A^{iy}/*a*) and A^{sy} (C57BL/6J-A^{sy}/*a*) were obtained from the Jackson Laboratory and mice carrying A^{vy} (AM/Wf-A^{vy}/a^m) were provided by the colony at the National Center for Toxicological Research (Jefferson, AR). These alleles are maintained in our laboratory by continued backcrossing to C57BL/6J-*a*/*a* mice, except for the A^{iy} mutation, for which A^{iy}/A^{iy} homozygotes were used for the RNA expression studies.

RNA expression and cDNA cloning studies. Total RNA obtained from tissues of adult mice was used for both northern hybridization and cDNA cloning studies. cDNA clones were derived using a PCR-based protocol for the "rapid amplification of cDNA ends"[25] (RACE) as described[19]. In brief, cDNA made with a primer from *agouti* exon 3, 5'–GAAACGGCACTGGCAGGAGG–3' was tailed with oligodC, and then PCR-amplified using a commercial "anchor primer" (Gibco-BRL) and an internal primer from exon 3, 5'–GGATTTCTTGTTCAGTGCCACG–3'. Positive clones were identified by colony hybridization using a probe specific for *agouti* exon 2. Except for A^{iy}2 for which only a single clone was isolated, multiple clones of similar length were isolated for each class of mutant cDNAs. The sequence of individual clones among each class was identical in the region of overlap except for one of the A^{vy} clones that exhibited a 2 bp difference in the region corresponding to exon 1A.

Analysis of genomic DNA in the A^{iy}, A^{sy} and A^{vy} alleles. The IAP insertions in A^{iy} and A^{vy} were cloned by amplifying A^{iy}/*a* or A^{vy}/*a* genomic DNA with oligonucleotide primers predicted to flank the insertion sites (Fig. 4, legend), using 30 cycles of the PCR with denaturation, annealing, and extension conditions of 94 °C/2 s, 55 °C/60 s, and 68 °C/600 s, respectively. The PCR was performed in a 50 µl volume using 2.5 U of *Taq* polymerase; 2.5 U of *Pfu* polymerase; 10% dimethylsulfoxide; and buffer conditions recommended by the supplier (Perkin-Elmer). For both A^{iy} and A^{vy}, large PCR products approximately 5.4 kb in length were visualized on agarose gels stained with ethidium bromide and were determined to contain an IAP by cross-hybridization with an IAP probe. In the case of A^{vy}, the large PCR product was isolated from the gel, cloned, and analysed by restriction mapping and partial DNA sequence analysis. In the case of A^{iy}, only the 3' LTR (with respect to the orientation of IAP transcription) and flanking genomic DNA was cloned and sequenced, and comparison to the 5' LTR insertion site was inferred from the A^{iy}1 cDNA sequence. The sequence of genomic DNA corresponding to the "pre-insertion site" for A^{iy} or A^{vy} was determined from genomic DNA cloned from the *A* allele.

The site of insertions for A^{iy}, A^{sy} and A^{vy} were also examined by Southern hybridization studies with A^{iy}/*a*, A^{sy}/*a*, A^{vy}/*a*, *a*/*a* and *A*/*A* genomic DNA using probes described in the legend to Fig. 5. The non-mutant restriction map (Fig. 5) is derived from cloned DNA of the *A* allele from the RIII strain, and does not differ from the Southern blot-based map of the *A* allele from the C3H/HeJ or the C57BL/6J strain except where noted in the legend to Fig. 5.

Received 13 February; accepted 11 July 1994.

Acknowledgements

We thank Sarah Millar for critical review of the manuscript. This work was supported in part by HG-00377 from the National Institutes of Health. H.V. is supported by the J.A. Cohen Institute, Leiden, The Netherlands. G.S.B. is an Assistant Investigator of the Howard Hughes Medical Institute.

1. Danforth, C.H. Hereditary adiposity in mice. *J. Hered.* **18**, 153–162 (1927).
2. Dickie, M.M. A new viable yellow mutation in the house mouse. *J. Hered.* **53**, 84–86 (1962).
3. Heston, W.E. & Vlahakis, G. Influence of the *A^{y}* gene on mammary-gland tumors, hepatomas, and normal growth in mice. *J. natn. Cancer Inst.* **26**, 969–982 (1961).
4. Heston, W.E. & Vlahakis, G. C3H-A^{vy}—a high hepatoma and high mammary tumor strain of mice. *J. natn. Cancer Inst.* **40**, 1161–1166 (1968).
5. Yen, T.T., Gill, A.M., Frigeri, L.G., Barsh, G.S. & Wolff, G.L. Obesity, diabetes, and neoplasia in yellow *A^{vy}/–* mice: Ectopic expression of the *agouti* gene. *FASEB J.* **8**, 479–488 (1994).
6. Silvers, W.K. The agouti and extension series of alleles, umbrous and sable. in *The Coat Colors of Mice* 6–44 (Springer-Verlag, New York, 1979).
7. Dickie, M.M. Mutations at the agouti locus in the mouse. *J. Hered.* **60**, 20–25 (1969).
8. Green, M.C. Catalog of mutant genes and polymorphic loci. in *Genetic Variants and Strains of the Laboratory Mouse* (eds Lyon, M.F. & Searle, A.G.) 17–20 (Osford University Press, Oxford, 1989).
9. Johnson, P.R. & Hirsch, J. Cellularity of adipose depots in six strains of genetically obese mice. *J. Lipid Res.* **13**, 2–11 (1972).
10. Wolff, G.L. Growth of inbred yellow (*A^{y}a*) and non-yellow (*aa*) mice in parabiosis. *Genetics* **48**, 1041–1058 (1963).
11. Wolff, G.L., Roberts, D.W. & Galbraith, D.B. Prenatal determination of obesity, tumor susceptibility, and coat color pattern in viable yellow (*A^{vy}/a*) mice. The yellow mouse syndrome. *J. Heredity* **77**, 151–158 (1986).
12. Hellerström, C. & Hellman, B. The islets of Langerhans in yellow obese mice. *Metabolism* **12**, 527–536 (1963).
13. Frigeri, L.G., Wolff, G.L. & Teguh, C. Differential responses of yellow A^{vy}/A and agouti A/a (BALB/c X VY) F1 hybrid mice to the same diets: glucose tolerance, weight gain, and adipocyte cellularity. *Int. J. Obes.* **12**, 305–30 (1988).
14. Dickerson, G.E. & Gowen, J.W. Hereditary obesity and efficient food utilization in mice. *Science* **105**, 496–498 (1947).
15. Hollifield, G. & Parson, W. Food drive and satiety in yellow mice. *Am. J. Physiol.* **189**, 36–38 (1957).
16. Shimizu, H., Shargill, N.S., Bray, G.A., Yen, T.T. & Geselichen, P.D. Effects of MSH on food intake, body weight and coat color of the yellow obese mouse. *Life Sci.* **45**, 543–552 (1989).
17. Yen, T.T., McKee, M.M. & Stamm, N.B. Thermogenesis and weight control. *Int. J. Obes.* **1**, 65–78 (1984).
18. Wolff, G.L. Influence of maternal phenotype on metabolic differentiation of agouti locus mutants in the mouse. *Genetics* **88**, 529–539 (1978).
19. Miller, M.W. *et al.* Cloning of the mouse agouti gene predicts a secreted protein ubiquitously expressed in mice carrying the Lethal-Yellow mutation. *Genes Devel.* **7**, 454–467 (1993).
20. Bultman, S.J., Michaud, E.J. & Woychik, R.P. Molecular characterization of the mouse agouti locus. *Cell* **71**, 1195–1204 (1992).
21. Michaud, E.J., Bultman, S.J., Stubbs, L.J. & Woychik, R.P. The embryonic lethality of homozygous lethal yellow mice (A(y)/A(y)) is associated with the disruption of a novel RNA-Binding protein. *Genes Devel.* **7**, 1203–1213 (1993).
22. Duhl, D.M.J. *et al.* Pleiotropic effects of the mouse *lethal yellow* (*A^{y}*) mutation explained by deletion of a maternally expressed gene and the simultaneous production of *agouti* fusion RNAs. *Development* **120**, 1695–1708 (1994).
23. Barsh, G.S., Lovett, M. & Epstein, C.J. Effects of the *lethal yellow* (*A^{y}*) mutation in mouse aggregation chimeras. *Development* **109**, 683–690 (1990).
24. Miller, M.W. *et al.* The mouse *lethal nonagouti* (*a^{x}*) mutation deletes the *S-adenosylhomocysteine hydrolase* (*Ahcy*) gene. *EMBO J.* **13**, 1806–1816 (1994).
25. Frohman, M.A., Dush, M.K. & Martin, G.R. Rapid production of full-length cDNAs from rare transcripts: amplification using a single gene-specific oligonucleotide primer. *Proc. natn. Acad. Sci. U.S.A.* **85**, 8998–9002 (1988).
26. Vrieling, H., Duhl, D.M.J., Millar, S.E., Miller, K.A. & Barsh, G.S. Differences in dorsal and ventral pigmentation result from regional expression of the mouse *agouti* gene. *Proc. natn. Acad. Sci. U.S.A.* **91**, 5667–5671 (1994).
27. Kozak, M. The scanning model for translation: an update. *J. Cell Biol.* **108**, 229–241 (1989).
28. Christy, R.J., Brown, A.R., Gourlie, B.B. & Huang, R.C. Nucleotide sequences of murine intracisternal A-particle gene LTRs have extensive variability within the R region. *Nucl. Acids Res.* **13**, 289–302 (1985).
29. Algate, P.A. & McCubrey, J.A. Autocrine transformation of hemopoietic cells resulting from cytokine message stabilization after intracisternal A particle transposition. *Oncogene* **8**, 1221–1232 (1993).
30. Kuff, E.L. & Lueders, K.K. The intracisternal A-particle gene family: structure and functional aspects. *Adv. Cancer Res.* 51, 183–276 (1988).
31. Horowitz, M., Luria, S., Rechavi, G. & Givol, D. Mechanism of activation of the mouse c-mos oncogene by the LTR of an intracisternal A-particle gene. *EMBO. J.* **3**, 2937–2941 (1984).
32. Christy, R.J. & Huang, R.C. Functional analysis of the long terminal repeats of intracisternal A-particle genes: sequences within the U3 region determine both the efficiency and direction of promoter activity. *Molec. cell. Biol.* **8**, 1093–102 (1988).
33. Heston, W.E. & Deringer, M.K. Relationship between the lethal yellow (*A^{y}*) gene of the mouse and susceptiblity to spontaneous pulmonary tumors. *J. natn. Cancer Inst.* **7**, 463–465 (1947).
34. Heston, W.E. & Vlahakis, G. Mammary tumors, plaques, and hyperplastic alveolar nodules in various combinations of mouse inbred strains and the different lines of the mammary tumor virus. *Int. J. Cancer* **7**, 141–148 (1971).
35. Vlahakis, G. & Heston, W.E. Increase of induced skin tumors in the mouse by the lethal yellow gene (*A^{y}*). *J. natn. Cancer Inst.* **31**, 189–195 (1963).
36. Wolff, G.L. *et al.* Tumorigenic responses to lindane in mice: potentiation by a dominant mutation. *Carcinogenesis* **8**, 1889–97 (1987).
37. Poznanski, A.A. & Calarco, P.G. The expression of intracisternal A particle genes in the preimplantation mouse embryo. *Dev. Biol.* **143**, 271–281 (1991).
38. Kuff, E.L. *et al.* Intracisternal A-particle genes as movable elements in the mouse genome. *Proc. natn. Acad. Sci. U.S.A.* **80**, 1992–1996 (1983).
39. Lueders, K.K., Frankel, W.N., Mietz, J.A. & Kuff, E.L. Genomic mapping of intracisternal A-particle proviral elements. *Mamm. Genome* **4**, 69–77 (1993).
40. Porter, S., Larue, L. & Mintz, B. Mosaicism of tyrosinase-locus transcription and chromatin structure in dark vs light melanocyte clones of homozygous chinchilla-mottled mice. *Dev. Genet.* **12**, 393–402 (1991).
41. Jackson, I.J. Molecular genetics. Colour-coded switches. *Nature* **362**, 587–588 (1993).
42. Conklin, B.R. & Bourne, H.R. Mouse coat colour reconsidered. *Nature* **364**, 110 (1993).